



HAL
open science

A high-resolution temporal framework to understand the reach-scale controls on wood budgeting

Borbála Hortobágyi, Stéphane Petit, Baptiste Marteau, Gabriel Melun, Herve
Piegay

► **To cite this version:**

Borbála Hortobágyi, Stéphane Petit, Baptiste Marteau, Gabriel Melun, Herve Piegay. A high-resolution temporal framework to understand the reach-scale controls on wood budgeting. 2024. hal-04642851

HAL Id: hal-04642851

<https://hal.science/hal-04642851>

Preprint submitted on 10 Jul 2024

HAL is a multi-disciplinary open access archive for the deposit and dissemination of scientific research documents, whether they are published or not. The documents may come from teaching and research institutions in France or abroad, or from public or private research centers.

L'archive ouverte pluridisciplinaire **HAL**, est destinée au dépôt et à la diffusion de documents scientifiques de niveau recherche, publiés ou non, émanant des établissements d'enseignement et de recherche français ou étrangers, des laboratoires publics ou privés.

26 **Informative title:**

27 A high-resolution temporal framework to understand the reach-scale controls on wood budgeting

28

29 **Running title:**

30 Hydrological control of wood budget

31

32 **Authors:**

33 Borbála Hortobágyi¹, Stéphane Petit², Baptiste Marteau¹, Gabriel Melun³, Hervé Piégay¹

34

35 **Affiliations:**

36 ¹ UMR5600 Environnement Ville Société, Université de Lyon, France

37 ² Véodis-3D, France

38 ³ Office français de la biodiversité, France

39

40 **Corresponding author:**

41 Borbála Hortobágyi

42 borbala.hortobagyi@ens-lyon.fr

43 UMR5600 Environnement Ville Société, Université de Lyon, UMR5600-EVS, ENS de Lyon Campus,
44 France

45

46

47 **Abstract**

48 Large active channels usually store more wood than channels with a narrow flow because of the
49 availability of large unvegetated bars for wood deposition and inner functioning that usually supplies
50 more wood through channel shifting. However, the dynamics of the wood supply (wood input, output,
51 or stability) can vary substantially over time and the drivers are largely unknown. To explore them, we
52 studied the temporal variability of large wood pieces and logjams along a 12-km reach of the lower
53 Allier River using six series of aerial images of variable resolution acquired between 2009 and 2020,
54 during which maximum river discharge fluctuated around the biannual (Q_2) flood magnitude. We show
55 that the wood budget was controlled by specific hydrological conditions. Wood output was best
56 explained by water levels exceeding bankfull discharge ($Q_{1.5}$). The duration of the highest magnitude
57 flood (over bankfull discharge) was the best predictor of wood inputs, with shorter floods resulting in
58 higher input rates. Finally, most of the wood remained stable when the river discharge did not exceed
59 60% of the bankfull discharge over a long period of time. Hydrological conditions driving jam build-up
60 and removal were similar to those controlling individual wood piece dynamics. A succession of floods
61 of similar (relatively low $\sim Q_2$) magnitude and decreasing flood duration since 2016 have probably
62 reinforced the filtering effect of wood obstacles, leading to positive feedback, which has been
63 strengthened by riparian vegetation colonisation of the active channel.

64

65 **Keywords**

66 large wood, temporal dynamics, hydrological factors, retention time, Allier River

67

68

69 1. Introduction

70 Human attitudes towards large wood in rivers are currently two-sided. On the positive side, in-channel
71 wood is seen as an essential element of riverine ecosystems, diversifying the physical habitat
72 conditions (e.g., flow velocity, grain size, temperature, and access to light) in a way that is valuable
73 for macroinvertebrates (Benke & Wallace, 2010) and fish species (Jones et al., 2014; Pettit et al.,
74 2013). Besides sediment storage, wood also provides considerable storage of carbon in river
75 floodplains (Wohl et al., 2012). Wood promotes landscape heterogeneity through its influences on
76 hydraulic conditions and hydrogeomorphic processes (e.g., sediment transport and deposition, shear
77 stress) in the channel and on alluvial bars (Gurnell et al., 2002; Gurnell & Sweet, 1998; Piégay &
78 Gurnell, 1997; Wohl, 2013). Moreover, in-channel wood also provides organic matter for the food
79 chain (Elosegi et al., 2007; Guiney & Lininger, 2022). On the negative side, wood is perceived as a
80 risk for infrastructure such as bridges and dams when individual pieces form obstructions (Ruiz-
81 Villanueva et al., 2014; Schmocker & Hager, 2011). Wood accumulation can also reduce the channel
82 section and induce a water level rise upstream from the jam, thereby increasing the upstream flood
83 risk. Wood jam-induced high water velocity around an obstacle leads to scouring and can increase
84 the fragility of infrastructure. Furthermore, large floating logs during floods can cause direct damage
85 to houses and other infrastructure (Le Lay et al., 2013).

86 Most of the wood stored in medium to large river corridors is recruited through lateral bank erosion,
87 and is strongly controlled by land cover (the availability of wood on the banks) (Iroumé et al., 2014;
88 Massé & Buffin-Bélanger, 2016), channel morphology, and hydrology (Gurnell & Petts, 2002; Piégay
89 et al., 1999). Wood recruitment has been studied at the local (Piégay & Marston, 1998) and watershed
90 scales (Boivin et al., 2017b), and over short interannual (Boivin et al., 2017a) to decadal time scales
91 (Lassetre et al., 2008).

92 The above mentioned studies and other works (e.g. Wohl & Cadol, 2011) emphasise the controlling
93 role of geomorphology in wood recruitment and wood storage. Once wood is recruited, logs are
94 transported downstream at various speeds and frequencies depending on their length and shape
95 (which effect resistance to flow), and their position within the catchment (e.g., the flow conditions
96 allowing transport are related to flow depth over space and time).

97 Model simulations by Ruiz-Villanueva et al. (2016) demonstrated that it is mainly water depth, rather
98 than surface roughness, that determines preferential sites for wood deposition in different geomorphic
99 units. Tree trunks can be deposited as individual pieces or they can form logjams (Piégay, 1993). A
100 single piece of wood is capable of trapping and stabilising other logs, and thereby initiating jam
101 development; this first element of the jam is called the “key member” (Abbe & Montgomery, 1996).

102 Wood stability is an important parameter for modelling and potentially preventing hazards associated
103 with large wood, although it can be difficult to assess. The transport rates reported in previous studies
104 show high variability, but the studies include a wide range of stream types, sizes, measurement
105 methods, and monitoring times. On large rivers, the mean annual transport rate is over 40% and can
106 exceed 80% (such as on the Tagliamento River in Italy) (Ruiz-Villanueva, Wyzga, et al., 2016). The
107 deposition of large pieces of wood and jams can have a high residence time counted in decades,
108 even reaching up to 200 years, and they can generate significant morphological changes (Keller &
109 Swanson, 1979). Wood tends to be more mobile in low gradient channels, but highly mobile large
110 pieces of wood and jams can also influence channel morphodynamics and downstream hydrology.
111 An example of relatively stable jams can be found in Australian ephemeral streams, where they are
112 key to driving geomorphic processes (Dunkerley, 2014). Gregory et al. (1985) demonstrated the role
113 of wood jams in slowing down the travel time of water, and thereby influencing a river's hydrography.
114 Individual wood pieces that become entwined within a jam obviously show much longer transit
115 durations than free pieces of wood (Kramer & Wohl, 2017). Jam size can fluctuate, with the episodic
116 release and capture of wood (Piégay et al., 2017). One of the elementary parameters determining
117 jam size is the size of the recruited trees or transported logs (Likens & Bilby, 1982). Hydrological
118 conditions drive retention of large wood (Galia et al., 2020), and also drive changes in the size of
119 jams. The retention of large pieces of wood in jams primarily occurs during normal flows (Hassan et
120 al., 2016). In a reach-scale analysis of the dynamics of large wood pieces in British Columbia, Hassan
121 et al. (2016) showed that an important proportion of the total accounted wood is stored within logjams.

122 Wood input and output at the reach-scale can be analysed using information gathered through
123 repeated field campaigns (Boivin et al., 2017a; Máčka et al., 2011), but such campaigns can be very
124 time-consuming and expensive, and are sometimes not possible to undertake for logistic or technical
125 reasons. Aerial imagery is an alternative that has been successfully used to determine wood storage
126 (Comiti et al., 2008; B. J. MacVicar et al., 2009; Ulloa et al., 2015) and monitor wood jam evolution
127 (Haschenburger & Rice, 2004), provided that the image resolution is sufficiently high (Marcus et al.,
128 2002). Galia et al. (2022) assessed spatiotemporal variations in large wood using satellite images and
129 found that it was not possible to make direct comparisons of volume and frequency through time
130 because of resolution differences across the images. Raft dynamics are easier to monitor using aerial
131 photographs or satellite images because of the greater spatial extent of rafts compared with individual
132 pieces (Boivin et al., 2015; Kramer & Wohl, 2015). Comiti et al. (2008) used aerial RGB images to
133 quantify wood storage within seven sub-reaches of braided/wandering rivers in Italy, while Smikrud
134 and Prakash (2006) used an automated method to map individual logs and wood accumulations to
135 assess changes in wood distribution over two successive years. Lassetre et al. (2008) used two
136 series of oblique aerial photographs, whereas Moulin et al. (2011) georeferenced video footage to

137 manually quantify individual trunks and jams within a 36-km reach of the Ain river (France). Atha
138 (2014) used 1-m-resolution satellite images from Google Earth to detect large wood over a broad
139 spatial scale. Riparian vegetation cover may obscure deposited wood, and therefore Atha (2013)
140 chose to manually interpret LiDAR point clouds. Methods such as supervised or automated
141 classifications were applied to hyperspectral and multispectral images for stream mapping (Leckie et
142 al., 2005; Marcus et al., 2002). Automated methods were also applied to LiDAR data and aerial four-
143 band imagery to quantify and measure individual wood pieces, although the failure to detect individual
144 trunks limited the success of the techniques (Richardson & Moskal, 2016). In addition, the data
145 sources used in these studies are costly and are rarely available at high frequency and over long
146 time-scales.

147 Even if we know both where wood is potentially coming from and the preferential sites for storage,
148 wood budgeting at the reach-scale remains a complex question: it is still difficult to predict when and
149 how much wood will arrive and depart from a specific river reach, as well as its duration of residency.
150 There is a crucial need to understand the processes controlling wood kinetics to calibrate algorithms
151 predicting wood mobility and improve modelling capabilities. Moreover, to provide adequate
152 management of large wood in large rivers, we need a good understanding of its dynamics from
153 recruitment to export. River discharge is the primary driver that governs wood transport (Gurnell et
154 al., 2002), and multiple studies have shown a significant correlation between peak flow magnitude
155 and wood export (Boivin et al., 2015; Moulin & Piégay, 2004; Ruiz-Villanueva, Piégay, et al., 2016;
156 Senter et al., 2017). However, the relationship appears to be nonlinear and slightly noisy (Boivin et
157 al., 2015; B. MacVicar & Piégay, 2012), demonstrating the complex interactions that exist between
158 the main channel, its margins and the alluvial plain in terms of wood exchange. Kramer and Wohl
159 (2017) suggested that a flow duration of near or just under bankfull discharge has the greatest
160 influence on the transport distance of large wood. One option to solve this issue is to develop a multi-
161 date analysis showing input and output under different hydrological contexts, thereby helping to obtain
162 an understanding of the main controlling factors.

163 Wood surveys at reach scale frequently concentrate on one dimension, particular the spatial
164 dimension of wood distribution (e.g., Andreoli et al., 2007; Galia et al., 2020; Massé & Buffin-Bélanger,
165 2016; Piégay & Marston, 1998), but are rarely performed over multiple timepoints. Reach-scale
166 studies that include temporal dynamics of wood are frequently undertaken within headwater reaches
167 or cover only short reach-lengths or time-scales, and sometimes do not make explicit links with
168 hydrological parameters (Daniels, 2006; Haschenburger & Rice, 2004; Iroumé et al., 2015; Jochner
169 et al., 2015; Latterell & Naiman, 2007; Wohl & Cadol, 2011; Wohl & Goode, 2008). A recent study
170 used hydrological proxies (discharge level, number of days exceeding geomorphologically significant
171 flow, accumulated geomorphic work) to explain channel morphodynamics and spatiotemporal

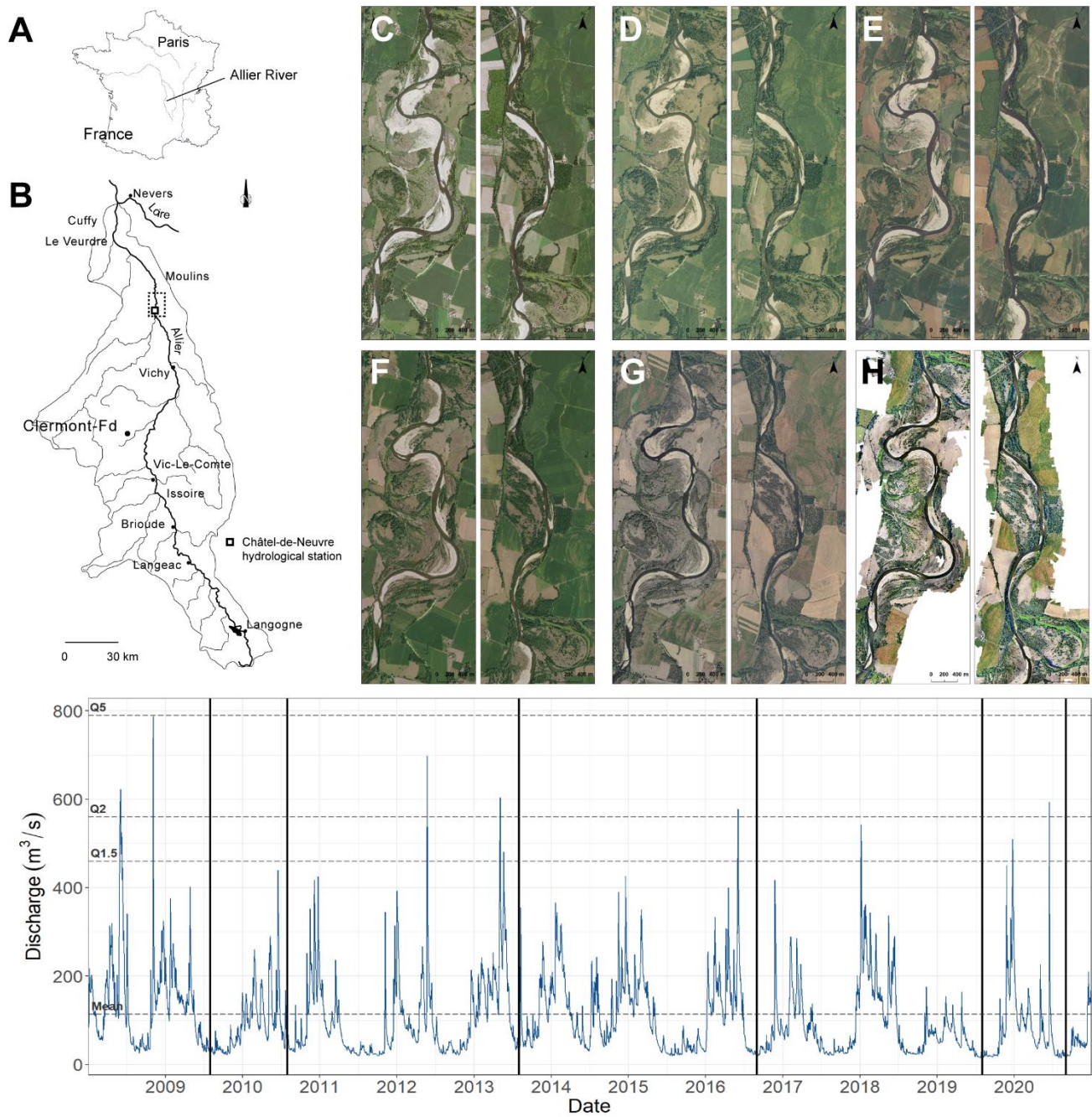
172 changes in the storage of large wood, but the focus was on intermittent Mediterranean rivers (Galia
173 et al., 2023). The use of tagging technologies to monitor individual wood pieces (Dixon & Sear, 2014;
174 Haga et al., 2002; Jochner et al., 2015; Ravazzolo et al., 2015; Schenk et al., 2014) has potential for
175 advancing our knowledge on the motion of wood, but it does not address long-term changes in inputs
176 and outputs of wood within the overall budget in relation to flow history.

177 Our aim with this paper is to achieve a better understanding of the drivers that control wood budgets
178 at the reach-scale, considering individual wood pieces and jams in terms of inter-annual inputs,
179 outputs, and stability. To accomplish this, we designed a comparative approach based on a high
180 frequency inter-annual survey strategy to evaluate geomorphological and hydrological factors
181 controlling wood input, output, and storage at the reach-scale. We applied our approach on a 12-km
182 reach of the Allier River in France because it is characterised by active lateral erosion and intense
183 exchanges of wood between the main channel and floodplain.

184 2. Methodology

185 *2.1. Study site and hydrological context*

186 The Allier River originates at 1485 m altitude, drains 14 400 km², and travels 410 km before joining
187 the Loire River at an altitude of 140 m (Figure 1A, B). The study area is located in the Natural Reserve
188 of Val d'Allier. This meandering reach of 12 km spans the length between the bridges of Châtel-de-
189 Neuvre and the N79 road. It is characterised by active shifting, with an average channel width of 60 m
190 (sd = 15) and a mean annual erosion rate between 0.2 and 0.9 ha/km/year (between 2009 and 2020).
191 The upstream section shows a higher channel migration rate than the downstream straighter section.
192 The hydrograph displays a strong seasonal pattern: the mean annual discharge at Châtel-de-Neuvre
193 where the Allier drains 12 430 km² is 114 m³/s, with Q₂ and Q₁₀ of 560 and 940 m³/s, respectively.



194

195 *Figure 1. (A) Location of the Allier River within France. (B) River basin of the Allier River and the*
 196 *location of the study reach within the dotted rectangle. (C)-(H) The six aerial images (2009, 2010,*
 197 *2013, 2016, 2019 and 2020) analysed to sense individual wood pieces and jams. The left image*
 198 *corresponds to the upstream part of the study site, the right one to the downstream part. (I) Mean*
 199 *daily discharge at Châtel-de-Neuvre. The dates of aerial images used for the analysis are indicated*
 200 *by vertical black lines.*

201 *2.2. Survey of wood input and output*

202 We used six series of aerial photographs (2009, 2010, 2013, 2016, 2019, and 2020) to analyse the
203 spatial distribution of large wood pieces (Figure 1C-H). Wood pieces were manually delineated on
204 each aerial image by drawing a line in ArcGIS (v10.0). We generated three groups of information from
205 the six maps: (i) the total number of wood pieces; (ii) the number of imported, exported, and stable
206 wood pieces at each date; and (iii) the retention time of each wood piece. Groups (ii) and (iii) were
207 estimated using the spatial join tool of ArcGIS.

208 *2.3. Survey of wood jams*

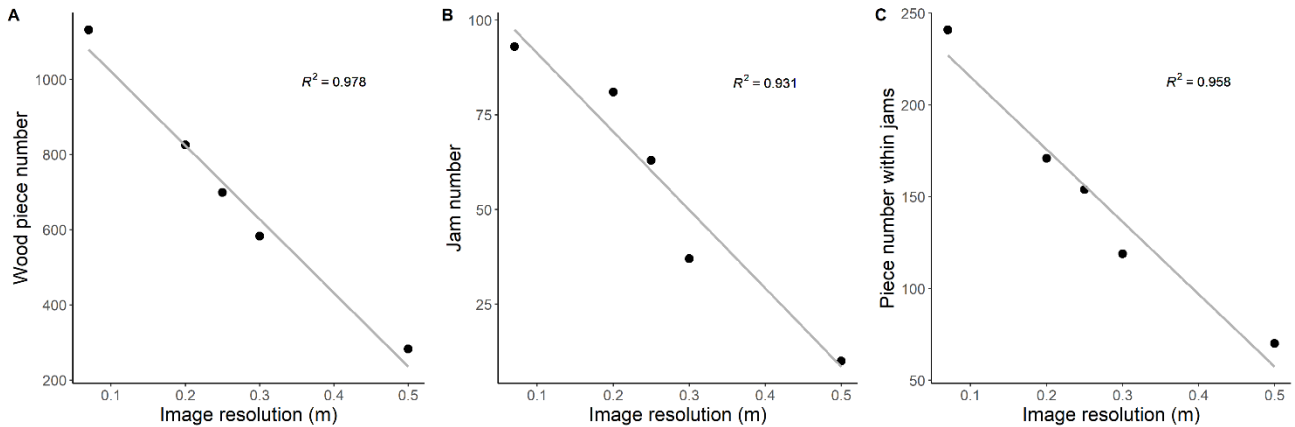
209 Jams were also quantified on the six series of aerial images, with a jam being defined as a wood
210 accumulation including at least three wood pieces (Ruiz-Villanueva, Piégay, et al., 2016). We
211 identified which jams had been created, destroyed, or were stable from one period to the next. In
212 addition to the number of jams present at each survey date, the number of wood pieces forming each
213 jam was quantified, providing an estimate of the growth or decline of stable jams. Stable jams were
214 considered to show size fluctuation when the decrease or increase in size was at least 50%, with this
215 definition being chosen to reduce possible quantification error and to focus on substantial changes.
216 The size of a jam was considered to be stable when the number of wood pieces at two consecutive
217 survey dates did not differ by more than +/- 3 pieces. This interval-based definition was used to
218 minimise reporting of false increase in jam size due to wood breakage within jam structures. The
219 proportion of wood stored within jams in relation to the total amount of wood quantified within the
220 reach was calculated for each survey date.

221 *2.4. Correction of image resolution bias for wood sensing*

222 The aerial photographs were acquired during low-flow periods and had a resolution varying from 0.5
223 to 0.07 m/pixel. Image resolution clearly affects the quantification of wood storage and results in
224 uncertainty in periodic comparisons of wood quantities. Instead of reducing the resolution of all images
225 to the lowest resolution, we first analysed images at their original resolution. Then, in a second step,
226 we reduced the resolution of the highest resolution 2020 image series to the lower resolutions of the
227 older series (e.g., 0.2, 0.25, 0.3, and 0.5 m/pixel). We selected a representative area within the
228 upstream dynamic section of the river that included alluvial bars, banks, and the main channel, and
229 the wood storage within this area was quantified for each decreased-resolution image of the 2020
230 series. The amount of wood pieces within this area represented close to 50 % of the total amount
231 found over the entire study area based on the original image of 2020. Comparisons between the
232 different resolutions revealed a linear relationship between image resolution and the number of

233 detected wood pieces (Figure 2A), which meant that a simple correction factor could be applied to
234 quantify changes in wood storage across the years.

235 The jam number and the number of wood pieces forming the jams were corrected in the same manner
236 as the total number of wood pieces, with both of these parameters showing a similar linear relationship
237 with resolution (Figure 2B, C).



238

239 *Figure 2. Relationship between aerial image resolution and (A) the number of wood pieces detected,*
240 *(B) the number of jams, and (C) the number of wood pieces forming jams.*

241 2.5. Hydrological conditions during the studied period

242 In 2008, the year before the earliest aerial image analysed, the river experienced a 5-year return-
243 period flood. The discharge was then very low between the first and second aerial images (2009–
244 2010). In 2012 and 2013, two 2-year floods occurred, and maximum discharge then decreased
245 between each study periods until the 2-year return-period flood of 2020 (Figure 1I).

246 Using this time series of flow discharge and imaging obtained at fixed timepoints, several hydrological
247 variables were derived from river discharge to explain wood budget variability. Ten hydrological
248 parameters and two parameters related to erosion processes were evaluated to determine the
249 conditions influencing the exported, imported, and stable wood quantities across periods. For each
250 period, the time over which the water discharge exceeded a given threshold or was within two
251 characteristic discharge levels was calculated. The parameters estimated in “hours” considered the
252 cumulative sum over the entire period between two aerial images, whereas the ones estimated in
253 “days” refer to individual floods that occurred during a given period. In this latter case, when more
254 than one flood occurred within a given period, only the peak flood was considered. The following
255 thresholds were used: mean annual discharge (114 m³/s), wood motion threshold (270 m³/s), bankfull
256 discharge (in this paper Q_{1.5} is used; 460 m³/s), and Q₂ (560 m³/s). The wood motion threshold was

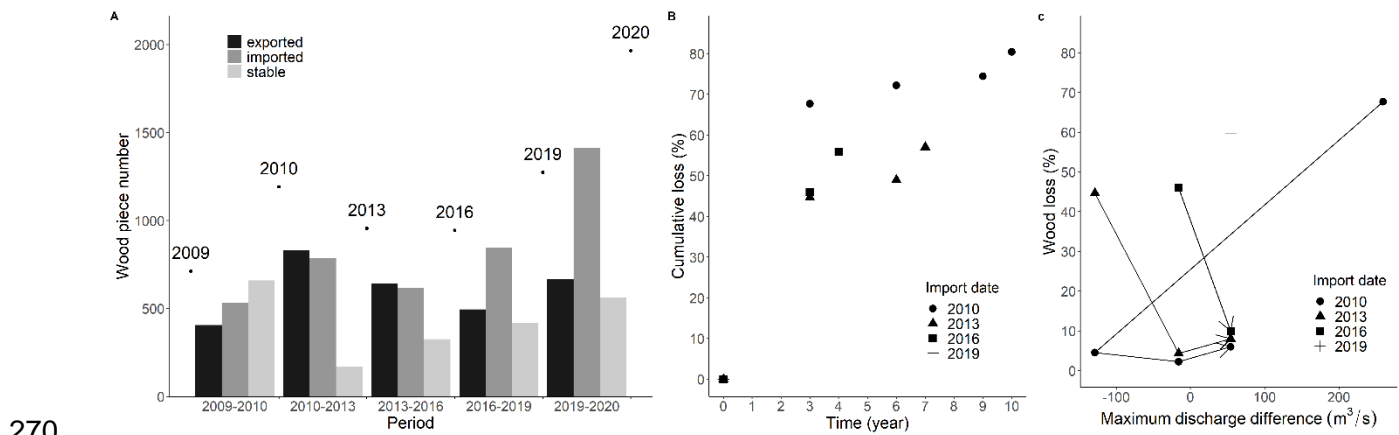
257 determined using video monitoring at Châtel-de-Neuvre. Cumulative energy was calculated by
 258 summing the discharge values during each of the rising limbs within a given period. In addition, the
 259 maximum discharge during the period and the total shrub- and forest-covered eroded surfaces (ha)
 260 were quantified. Pearson correlations were performed to test which of the eleven parameters
 261 modulated wood input and output, jam stability, and the amount of wood in jams. R software (R Core
 262 Team, 2022) was used for this analysis.

263 3. Results

264 3.1. Temporal changes in the storage of individual wood pieces

265 3.1.1. Inter-annual change in storage of individual wood pieces

266 The corrected number of individual wood pieces detected varied between 712 (2009) and 1966
 267 (2020), corresponding to 59 and 164 trunks per km of river, respectively. The number of wood pieces
 268 increased from 2009 to 2010, decreased between 2010 and 2016, then increased again from 2016
 269 to 2020 (Figure 3).



270

271 *Figure 3. (A) Total number of wood pieces per year (dots), and number of exported, imported, and*
 272 *stable wood pieces per period (bars), all corrected for resolution bias. (B) Cumulative wood loss in*
 273 *relation to time (100% = all imported wood over a given time). (C) Relative change in wood loss (100%*
 274 *= all imported wood over a given time) in relation to the difference in maximum discharge between*
 275 *successive periods.*

276 The amount of imported wood pieces was always higher or very similar to the exported amount (Figure
 277 3). The periods 2016–2019 and 2019–2020 were the most favourable for wood import. Between 2013
 278 and 2016, wood import and export were approximately balanced. Wood export increased from 2010
 279 to 2013, then decreased until 2019, when it then increased again. The highest wood export occurred

280 in 2013. Between 2009 and 2010, a higher number of wood pieces remained stable than were either
281 imported or exported. The amount of stable wood pieces then increased progressively from 2013
282 onwards.

283 3.1.2. River discharge as a parameter for predicting storage of individual wood 284 pieces

285 The best explanatory variables for the number of stable wood pieces were the cumulative number of
286 hours when the discharge exceeded 60% of bankfull discharge ($r = -0.99$; $p\text{-value} < 0.005$) and
287 cumulative energy ($r = -0.98$; $p\text{-value} < 0.005$; Table 1, Figure 4A, B), with both variables showing
288 negative correlations. There were also significant and strong negative correlations with erosion rate
289 and vegetated eroded surface (Table 1, Figure 4C, D). The parameters best-explaining wood export
290 were maximum discharge ($r = 0.96$; $p\text{-value} < 0.05$), the cumulative number of hours when the
291 discharge exceeded bankfull discharge ($r = 0.98$; $p\text{-value} = 0.005$), and erosion rate ($r = 0.95$; $p\text{-value} < 0.05$;
292 Table 1, Figure 4E, F, G). The only parameter showing a significant association with the
293 amount of imported wood was the duration of individual floods (the highest flood if multiple floods
294 occurred) higher than bankfull discharge ($r = -0.99$; $p\text{-value} < 0.05$; Table 1, Figure 4H). Note that
295 only four points are presented in Figure 4H because the flow did not exceed bankfull discharge in
296 2010. The longest floods above bankfull discharge occurred in 2013 and 2016 (both 4 days; Figure
297 4I). For the periods of 2010–2013 and 2019–2020, the highest floods were used when performing the
298 correlations, although these floods were not the ones with the longest duration (3 days and 1 day,
299 respectively). The 2018 flood had a slightly lower magnitude than the one in 2016, which lasted one
300 day longer, but it imported more wood and exported less wood than the flood in 2016. In contrast, the
301 2012 and 2018 floods had the same duration but showed a large difference in magnitude ($Q_{2012} >$
302 $Q_2 > Q_{2018}$, see Figure 1I, Figure 4I).

303

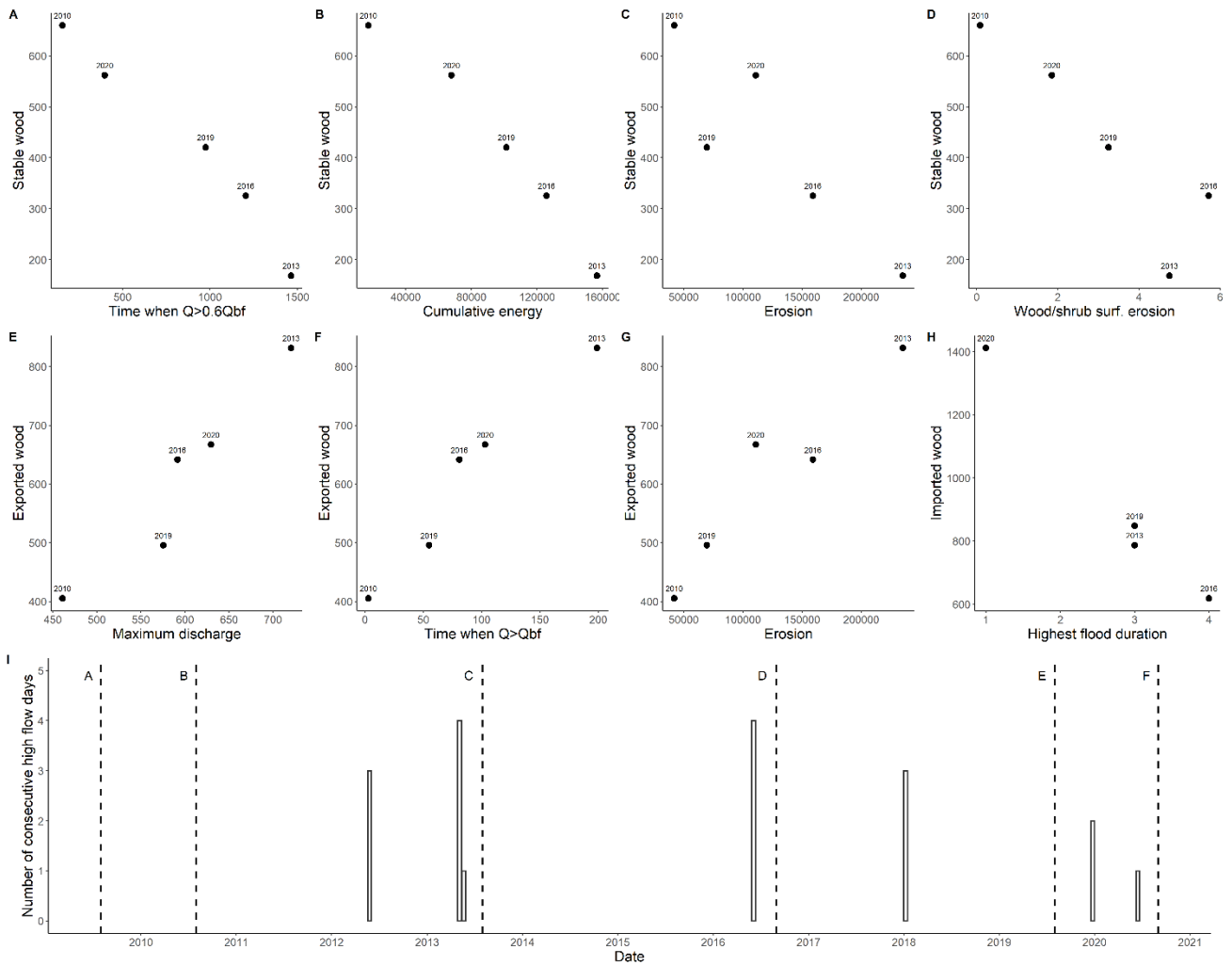
304 Table 1. Pearson correlation coefficients (and p-values) between the tested hydrological parameters and (i) the amount of stable, exported, and
 305 imported wood, (ii) the stable, destroyed, and created jams and (iii) the proportion of wood pieces forming the jams (100% = total number of wood
 306 pieces per year).

307 † Cumulative values computed for the entire study periods

308 ‡ Values were calculated individually for each flood and only the highest flood was used for the correlation if multiple floods occurred over the study period.

Type	Dynamic	Max discharge [†]	Duration over which discharge exceeded mean annual discharge [†]	Duration over which discharge exceeded bankfull discharge [†]	Duration over which discharge exceeded 60% of bankfull discharge [†]	Duration over which discharge was between mean annual and bankfull discharge [†]	Duration over which discharge exceeded Q ₂ discharge [†]	Cumulative energy [†]	Erosion (ha) [†]	Eroded shrub and forest surface (ha) [†]	Flood duration above a threshold of 270 m ³ /s [‡]	Flood duration above a threshold of bankfull discharge [‡]
Individual wood	Stable	-0.8 (0.100)	-0.8 (0.090)	-0.8 (0.093)	-0.99 (<0.005)	-0.8 (0.096)	-0.9 (0.126)	-0.98 (<0.005)	-0.9 (<0.05)	-0.9 (<0.05)	-0.6 (0.288)	-0.7 (0.312)
	Exported	0.96 (<0.05)	0.5 (0.438)	0.98 (0.005)	0.7 (0.198)	0.4 (0.453)	0.9 (0.093)	0.8 (0.105)	0.95 (<0.05)	0.7 (0.225)	0.0 (0.970)	-0.1 (0.935)
	Imported	0.4 (0.475)	-0.5 (0.449)	0.3 (0.620)	-0.2 (0.740)	-0.5 (0.439)	-0.4 (0.571)	-0.0 (0.973)	0.0 (0.956)	-0.2 (0.815)	-0.6 (0.297)	-0.99 (<0.05)
Jam	Stable	-0.7 (0.210)	-0.7 (0.158)	-0.8 (0.134)	-0.9 (<0.05)	-0.7 (0.165)	-0.9 (0.090)	-0.9 (0.068)	-0.9 (0.056)	-0.7 (0.154)	-0.5 (0.388)	-0.6 (0.392)
	Destroyed	0.8 (0.084)	0.1 (0.903)	0.9 (<0.05)	0.4 (0.478)	0.1 (0.922)	0.8 (0.221)	0.5 (0.367)	0.8 (0.109)	0.3 (0.675)	-0.3 (0.611)	-0.3 (0.716)
	Created	-0.3 (0.623)	-0.95 (<0.05)	-0.3 (0.612)	-0.9 (0.058)	-0.95 (<0.05)	-0.5 (0.522)	-0.8 (0.134)	-0.5 (0.348)	-0.9 (0.067)	-0.9 (<0.05)	-0.99 (<0.05)
Proportion of wood pieces forming the jams	-	-0.3 (0.636)	-0.2 (0.733)	-0.3 (0.574)	-0.1 (0.923)	-0.2 (0.740)	-0.96 (<0.05)	-0.2 (0.781)	0.2 (0.692)	0.4 (0.523)	0.2 (0.768)	-0.1 (0.837)

309



310

311 *Figure 4. Relationships between: the number of stable wood pieces and (A) the cumulative time*
 312 *(hours) over which discharge exceeded 60% of bankfull discharge, (B) cumulative energy, (C) erosion*
 313 *rate, (D) eroded wood/shrub surface; between the number of exported wood pieces and (E) the*
 314 *maximum discharge, (F) cumulative time (hours) over which discharge exceeded bankfull discharge,*
 315 *and (G) erosion rate; and between (H) the number of imported wood pieces and the duration of the*
 316 *highest flood (in days) above of bankfull discharge. (I) Duration of all floods above bankfull discharge.*

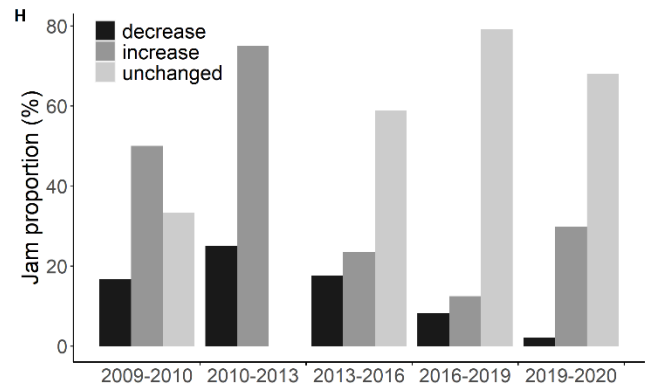
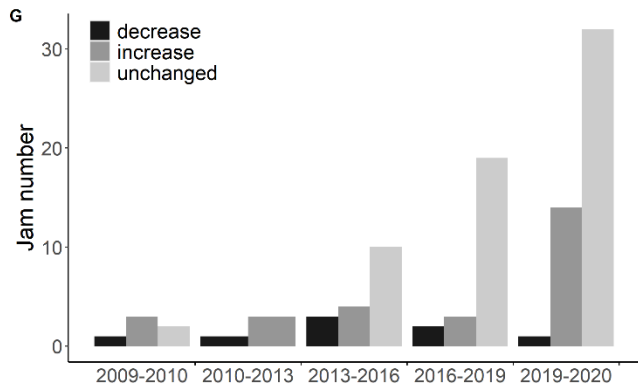
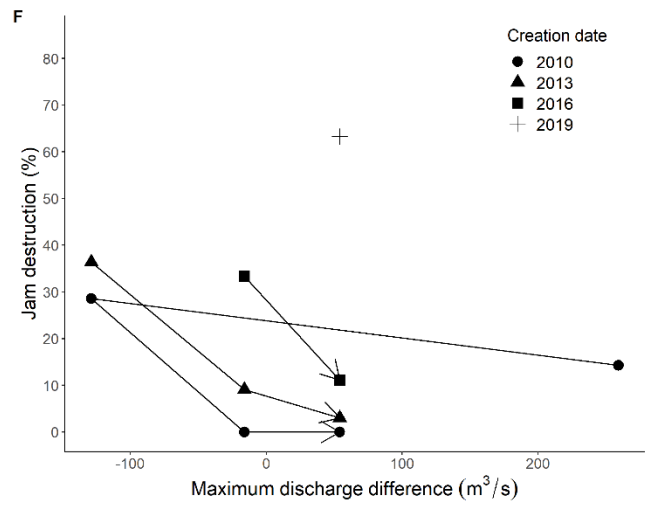
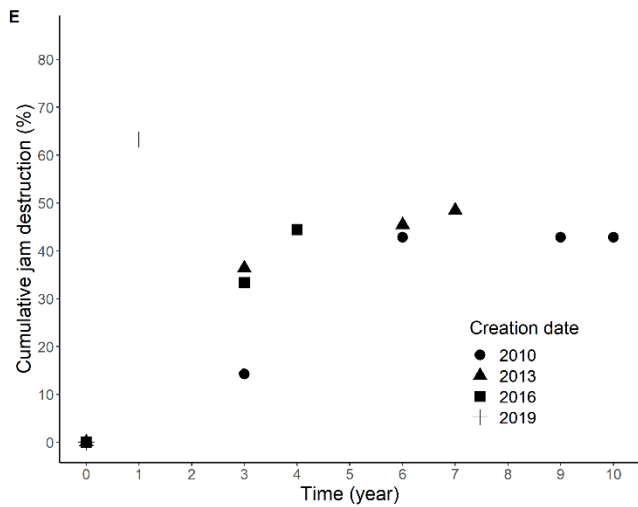
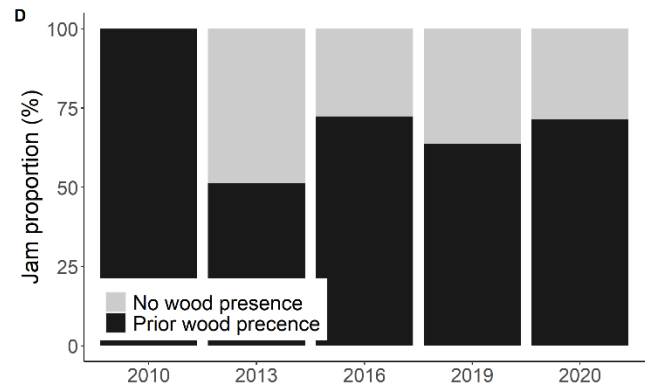
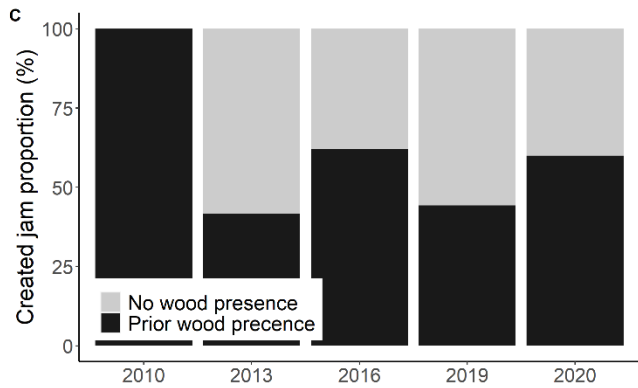
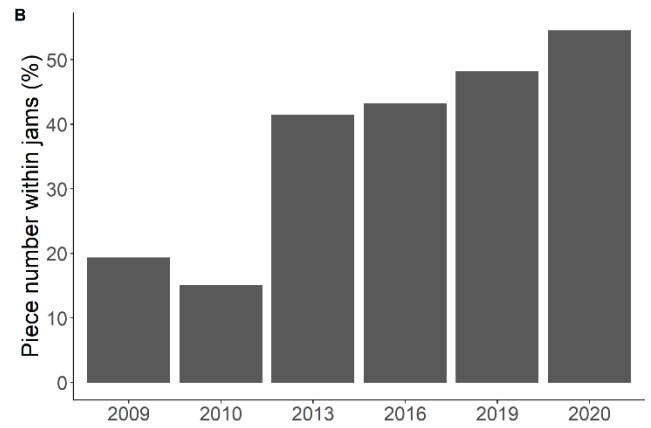
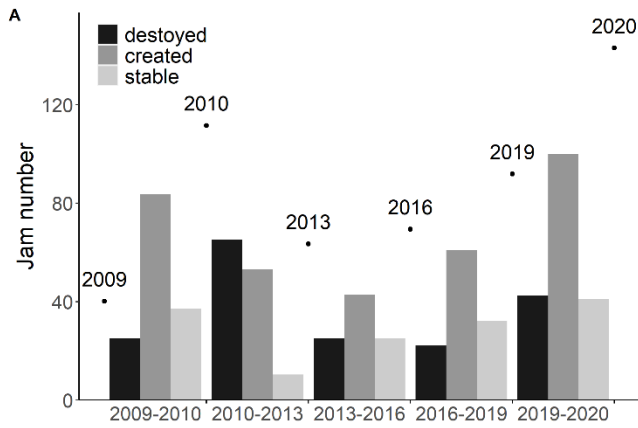
317 We analysed the arrival year and export year of each wood pieces to quantify how fast imported wood
 318 was exported from the reach and how long it remained within the reach. We found that between 45%
 319 and 68% of wood pieces were straight away remobilised within one to three years (Figure 3B) and
 320 that 20% of the wood imported in 2010 and approximately 40% of the wood imported in 2013, 2016,
 321 and 2019 remained stationary. The proportion of imported wood that was remobilised was much
 322 higher (over 40%) during the period immediately succeeding a deposition phase than in following
 323 periods (below 10%) (Figure 3B). Between 56% and 80% of imported wood was exported before the
 324 last studied period. Maximum discharge influenced how fast the imported wood was remobilised. The
 325 changes in imported wood over time were dependent on the relative magnitude of successive floods.

326 Wood loss remained below 50% (45% and 46% of the import in 2013 and 2016, respectively) when
327 maximum discharge was lower than the peak flow of the preceding period, and over 50% (60% and
328 68% of the import in 2019 and 2010, respectively) when maximum discharge exceeded the peak
329 discharge that occurred during the preceding period (Figure 3C). Thus, a relative negative discharge
330 balance ($Q_{\max}^t > Q_{\max}^{t+1}$) also resulted in lower wood loss (in 2010 and 2013) than the opposite
331 situation ($Q_{\max}^t < Q_{\max}^{t+1}$, in 2016). Wood loss increased when a positive discharge balance followed
332 a negative one (the last period of import in 2010 and 2013).

333 *3.2. Temporal changes in wood jams*

334 3.2.1. Inter-annual change in wood jam storage

335 The corrected number of jams per survey date varied between 40 (2009) and 144 (2020),
336 corresponding to 3.3 and 12 jams per km of river, respectively. The number of jams increased from
337 2009 to 2010, decreased between 2010 and 2013, then increased again from 2013 to 2020 (Figure
338 5A).



340 *Figure 5. (A) Total number of jams per year (dots) and number of destroyed, created, and stable jams*
341 *per period (bars), corrected for resolution bias. (B) The proportion of wood stored within jams in*
342 *relation to the total amount of wood quantified within the reach at each survey date. (C) Proportions*
343 *of newly built (created) jams with and without prior wood presence. (D) Proportions of all jams with*
344 *and without prior wood presence. (E) Cumulative jam destruction in relation to time (100% = all jams*
345 *created over a given duration). (F) Relative change in jam destruction (100% = all imported jams over*
346 *a given time) in relation to the difference in maximum discharge between successive periods. Size*
347 *fluctuation of stable jams represented as (G) absolute values and (H) as relative proportion for the*
348 *period.*

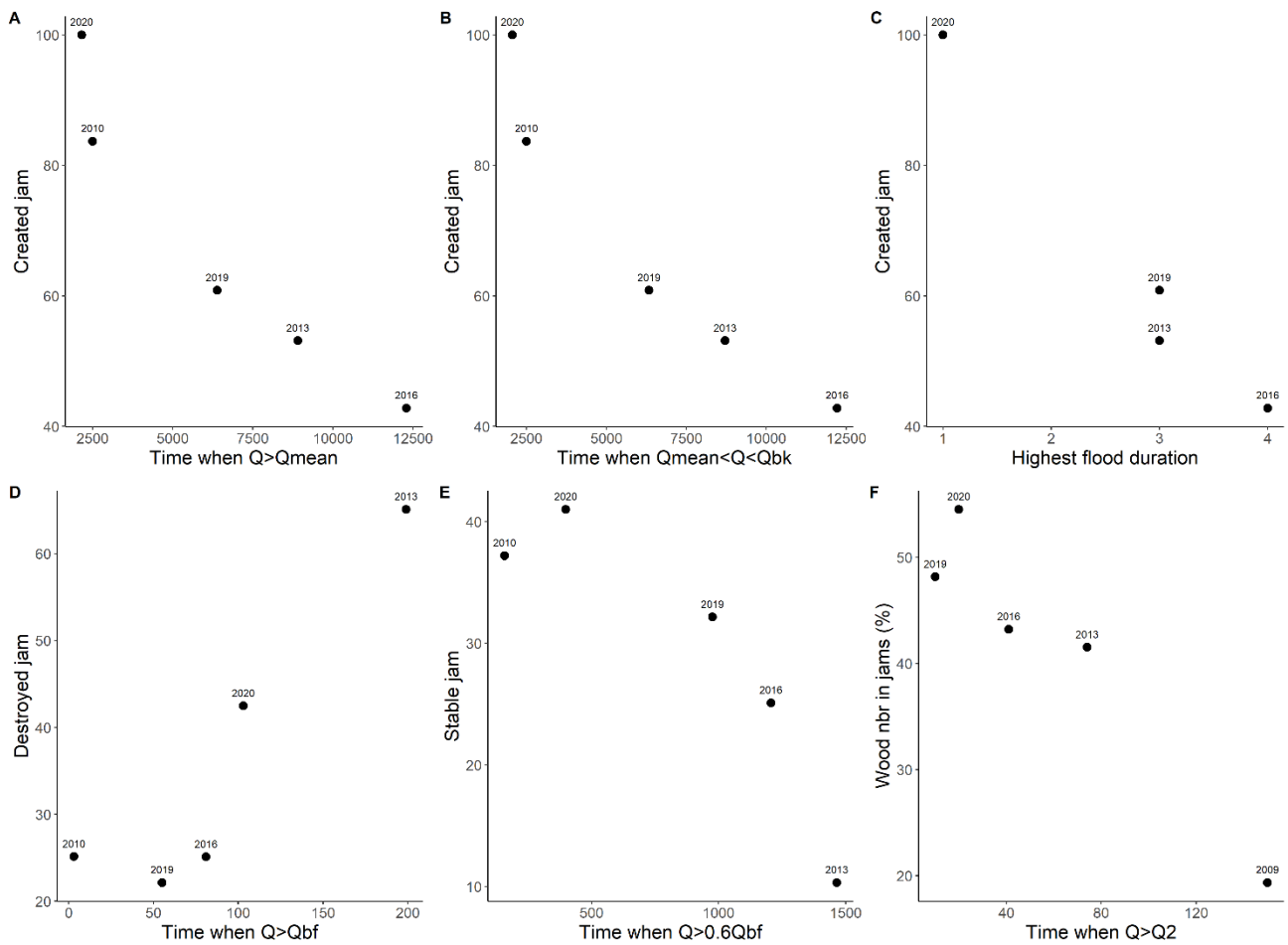
349 The number of jams created was higher than the number of destroyed ones, except during the period
350 2010–2013 (Figure 5A). The periods 2009–2010 and 2019–2020 were the most favourable for jam
351 formation. Jam destruction was highest over the periods 2010–2013 and 2019–2020. The number of
352 stable jams was highest during the first and last studied periods.

353 Jams can build up on bare surfaces or because of obstacles such as riparian vegetation, man-made
354 structures, and previous wood deposits. We computed the proportions of jams built over a given
355 period that occurred with or without wood being previously present (Figure 5C). The proportions
356 estimated for 2013, 2019, and 2020 were probably underestimated because the lower image
357 resolution of the previous year's imaging resulted in lower detection of wood. Unfortunately, this error
358 cannot be corrected. We estimated the proportions of new jams that were built on a key member (an
359 already present wood piece) to be 100% in 2010, >40% in 2013, 62% in 2016, >43% in 2019, and
360 >60% in 2020. These results indicate that deposited wood plays a facilitating role in jam formation.
361 Even at floods higher than the biannual maximum (2013), 40% of created jams formed where at least
362 one wood piece was present. The proportion of jams that were built on a key member accounted for
363 at least 43% following biannual floods (2016, 2019, 2020). When all jams measured on an aerial
364 image were considered (newly created and previously existing), at least 51% of jams were built on a
365 key member (Figure 5D). The proportion of wood stored within jam structures increased from 2010
366 (Figure 5B). Over 2010 to 2013, the proportion more than doubled, reaching 42%. From 2013 it then
367 increased gradually, reaching 55% in 2020.

368 3.2.2. River discharge as a parameter for predicting storage of wood in jams

369 The number of jams created correlated strongly with the duration over which discharge exceeded
370 mean annual discharge, the duration over which discharge was between mean annual and bankfull
371 discharge (for both: $r = -0.95$; $p\text{-value} < 0.05$), and the duration over which the flood was above a
372 threshold of bankfull discharge ($r = -0.99$; $p\text{-value} < 0.05$) (Table 1, Figure 6A, B, C). There was also
373 a significant negative correlation with the duration of flooding above a threshold of $270 \text{ m}^3/\text{s}$, but the
374 relationship was not as strong. The parameter that best explained jam destruction was the cumulative

375 number of hours over which the discharge exceeded bankfull discharge (for both: $r = 0.9$; p -
 376 value < 0.05) (Table 1, Figure 6D). The variable best explaining stable jams was the cumulative
 377 number of hours over which the discharge exceeded 60% of bankfull discharge ($r = -0.9$; p -
 378 value < 0.05) (Table 1, Figure 6E). The changes in the proportion of jammed wood could be explained
 379 by the duration over which the discharge exceeded the biannual discharge ($r = -0.96$; p -value < 0.05)
 380 (Table 1, Figure 6F).



381

382 *Figure 6. Relationships between: the number of created jams and (A) the cumulative time (hours)*
 383 *over which discharge exceeded mean annual discharge, (B) the cumulative time (hours) over which*
 384 *the discharge was between the mean annual discharge and the bankfull discharge, and (C) the*
 385 *duration over which the highest flood (in days) was above bankfull discharge; between (D) the amount*
 386 *of destroyed jams and the cumulative time (hours) over which discharge exceeded bankfull discharge;*
 387 *(E) between the number of stable jams and cumulative time (hours) over which discharge exceeded*
 388 *60% of bankfull discharge; (F) between the proportional number of wood pieces forming jams (100%*
 389 *= total number of wood pieces per year) and the cumulative time (hours) over which discharge*
 390 *exceeded the biannual discharge.*

391 We also analysed the dynamics of each jam (i.e., the creation year and the destruction year) to
 392 quantify how fast the created jams were destroyed or how long they remained in place. We observed

393 large differences in the proportion of jams being destroyed within one or three years, with the
394 proportion ranging from 14% to 63% (Figure 5E). A higher proportion of jams (over 30%) were
395 remobilised directly after their build-up (i.e., within one or three years) than during later periods (within
396 6-10 years; approximately 10%), as in the cases of jam creation in 2013 and 2016. However, the
397 temporal trajectory of the jams created in 2010 was different: fewer jams were destroyed over the first
398 period (14%) than over the second period (29%), although it is important to note that the numbers of
399 jams represented by these percentages were very low (1 and 3, respectively). Approximately 55% of
400 the jams created in 2010, 2013, and 2016, and 40% of the jams created in 2019, were still in place at
401 the end of the study period. The destruction of jams in relation to discharge balance was similar to
402 that of individual wood pieces, with the exception of 2010 (Figure 5F). A negative discharge balance
403 during the first remobilisation period resulted in lower wood loss than the positive discharge balance.
404 However, contrary to the pattern for individual wood pieces, when a positive discharge balance
405 followed a negative one, the proportion of jams destroyed decreased, or at least no further jam
406 destruction occurred (the latest import period of 2010 and 2013).

407 As explained above, jams could stay in place for several years. Over this time, their size could
408 fluctuate or stay unchanged. Figure 5G, H represents the size fluctuation of stable jams that showed
409 a variation in size of at least 50%. The first two periods are not representative because there were
410 only six or four jams per period. From 2013, most of the stable jams did not vary in size (at least 60%),
411 and fewer jams decreased in size. The highest size increase was observed over the period 2019–
412 2020, and the lowest over the period 2016–2019.

413 4. Discussion

414 *4.1. Methodology*

415 We showed that accessible resources in the form of aerial photographs can provide valuable
416 information on changes in wood amounts at a reach scale if differences in image resolution are
417 carefully considered and relative proportions are used rather than absolute values. The bias related
418 to image resolution can be easily overcome, and we propose a correction coefficient that can be used
419 for future analysis using aerial imagery with a resolution between 0.07 and 0.5 m/pixel. This
420 methodology could also be applied to assess the spatiotemporal dynamics of large wood pieces from
421 satellite images, thereby bypassing the resolution issues mentioned by Galia et al. (2023).

422 In addition to low resolution, other parameters can interfere with wood detection and inter-annual
423 analysis of wood budgets. Vegetation can limit wood detection when it grows on or overhangs wood
424 deposits, such as on alluvial bars and banks. Thus, the retention time can be underestimated and

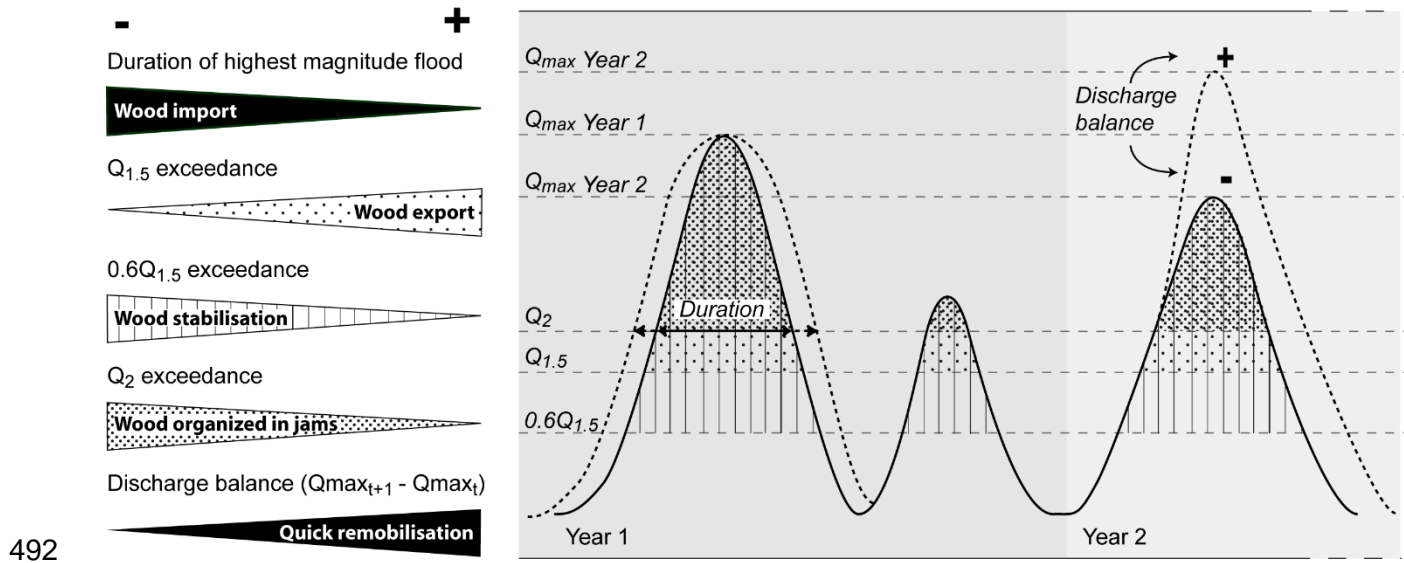
425 wood export overestimated. For alluvial bars, a solution would be to integrate vegetation cover into
426 the analysis as an indicator of stability. Between 2013 and 2016, we observed relatively important
427 vegetation growth on alluvial bars, resulting in false negative detections. Export appeared more
428 important than it really was because of vegetation development and growth.

429 *4.2. Discharge as a factor controlling wood storage over time*

430 Studies on the frequencies of individual wood jams report large variability in storage over space and
431 time. On a 36-km-long reach of the meandering Ain River, Lassettre et al. (2008) observed
432 frequencies of 20 and 43 pieces of wood per km at different timepoints, locally attaining 72 pieces per
433 km. On the Allier River, wood storage can be three times higher (71–202 trunks/km). A likely
434 explanation for this is the higher volume of wood recruited through lateral erosion: 17–36 m³/km/year
435 on the Ain River vs. 58 m³/km/year on the Allier River. In comparison, Moulin et al. (2011) performed
436 a georeferenced aerial survey on a meandering river in the U.S. and found 55 individual wood
437 pieces/km and 59 pieces/km forming jams, giving a total of 114 trunks/km. On an intermittent
438 Mediterranean river, between 7.7–23.9 pieces/km and 0.4–11 jams/km were observed using 0.5-m
439 resolution satellite imagery (Galia et al., 2023). Piégay and Landon (1997) observed up to 36–40
440 individual wood pieces/500 m on the Drôme river. The jam frequency on the Allier River is between
441 3.3 and 12 jams/km. In comparison, Dunkerley (2014) measured (in the field) 3 jams/km on the
442 Fowlers Creek ephemeral river, and great spatial and temporal variability (0.9–4.1 jams/km) in jams
443 was observed on the low gradient San Antonio River in Texas (Curran, 2010). Field surveys on the
444 Gregory and Riley creeks (British Columbia), where wood recruitment is dominated by mass
445 movement and bank erosion, found 6 and 8.8 jams/km (Hassan et al., 2016). Because we know that
446 the detection rate of remotely sensed data has a resolution that is significantly lower than observed
447 field data, the remote sensing performed on the Allier shows that the amount of wood stored is fairly
448 high.

449 Multiple factors control wood recruitment and storage in rivers, including (i) the availability of riparian
450 vegetation, (ii) channel patterns, and (iii) river flow (Lassettre et al., 2008). In this study, we focussed
451 on testing river discharge as a factor controlling wood jams and storage within a channel reach. The
452 proportions of wood and jam inputs and outputs varied over the study period; thus, the factors
453 controlling the two aspects probably differ. This is in line with the asynchronous wood import and
454 export observed over a 10-year period within small low-order reaches in Chile (Iroumé et al., 2020).
455 The relationship between peak flows and wood export described in previous studies at the basin scale
456 (Moulin & Piégay, 2004; Ruiz-Villanueva et al., 2019) seems to also be observed when studying wood
457 budgets at the reach-scale. Higher maximum discharges result in higher amounts of wood export.
458 However, wood export correlates best with the duration over which discharge exceeds bankfull

459 discharge. This also corresponds to the discharge condition that facilitates jam removal. Observations
460 on Chilean low-order rivers also suggested higher large wood mobility when flow discharge exceeds
461 bankfull discharge (Iroumé et al., 2015). Gregory et al. (1985) monitored wood jams over a year on a
462 small river in England. Over that period, one high-flow event approached bankfull discharge and
463 removed 36% of the jams. Probably the most similar hydrological conditions observed on the Allier
464 River were those between 2009 and 2010, when it had a slightly higher (40%) jam removal rate. The
465 duration of the highest magnitude flood (over bankfull discharge) was found to be the best predictor
466 of wood import and the occurrence of new jams. When the water level exceeds the statistical bankfull
467 discharge ($Q_{1.5}$) over a long period, wood import and jam build-up decrease. Most wood pieces and
468 jams remained stable when river discharge remained below 60% of bankfull discharge over a long
469 period of time. Analysis of video recordings of the Ain river allowed quantification of the wood motion
470 threshold, which is approximately when discharge reaches that threshold (Ghaffarian et al., 2020; B.
471 MacVicar & Piégay, 2012). Our results are in line with this finding because the amount of stabilised
472 wood on the Allier River decreased when the number of days exceeding $0.6 Q_{bf}$ during a given period
473 increased. Thus, these three hydrological conditions ($Q > Q_{bf}$, duration of the highest magnitude flood,
474 and $0.6 Q_{bf}$) can determine the mobility of individual wood pieces and jams at the same time, which
475 tend to fluctuate in parallel. This means that there are two critical discharge levels: bankfull discharge
476 and the $0.6 Q_{bf}$ threshold (Figure 7). A discharge over bankfull level over a relatively long period is
477 necessary to activate wood export, and also to promote individual log deposition. Between 2009 and
478 2010, the mean daily discharge did not exceed bankfull discharge, resulting in the lowest import of
479 individual wood pieces and the only period over which more wood pieces remained stable than were
480 either imported or exported (i.e., low dynamism). However, this was not the case for logjams, because
481 we recorded the second highest jam creation rate over the same period. All the newly formed jams
482 were built around so-called key members. We hypothesise that the high magnitude flood of 2009 (Q_5)
483 left easily accessible wood that could be transported, even by such a low magnitude flood as the one
484 in 2010. This wood was mostly filtered out of the flow by existing logs located at low elevation, and
485 therefore, compared with other periods, proportionally more new jams were formed than isolated
486 deposits. Kramer and Wohl (2017) hypothesised that the greatest influence on large wood transport
487 distance was the flow duration near or just under bankfull discharge, and also suggested that a shorter
488 travel distance due to shorter floods can lead to increasing jam build-up. Whether wood is organised
489 within jams or deposited as isolated pieces seems to depend on discharge conditions; wood has an
490 increasing tendency to be organised into jams when the cumulative time with discharge above Q_2 is
491 shorter.



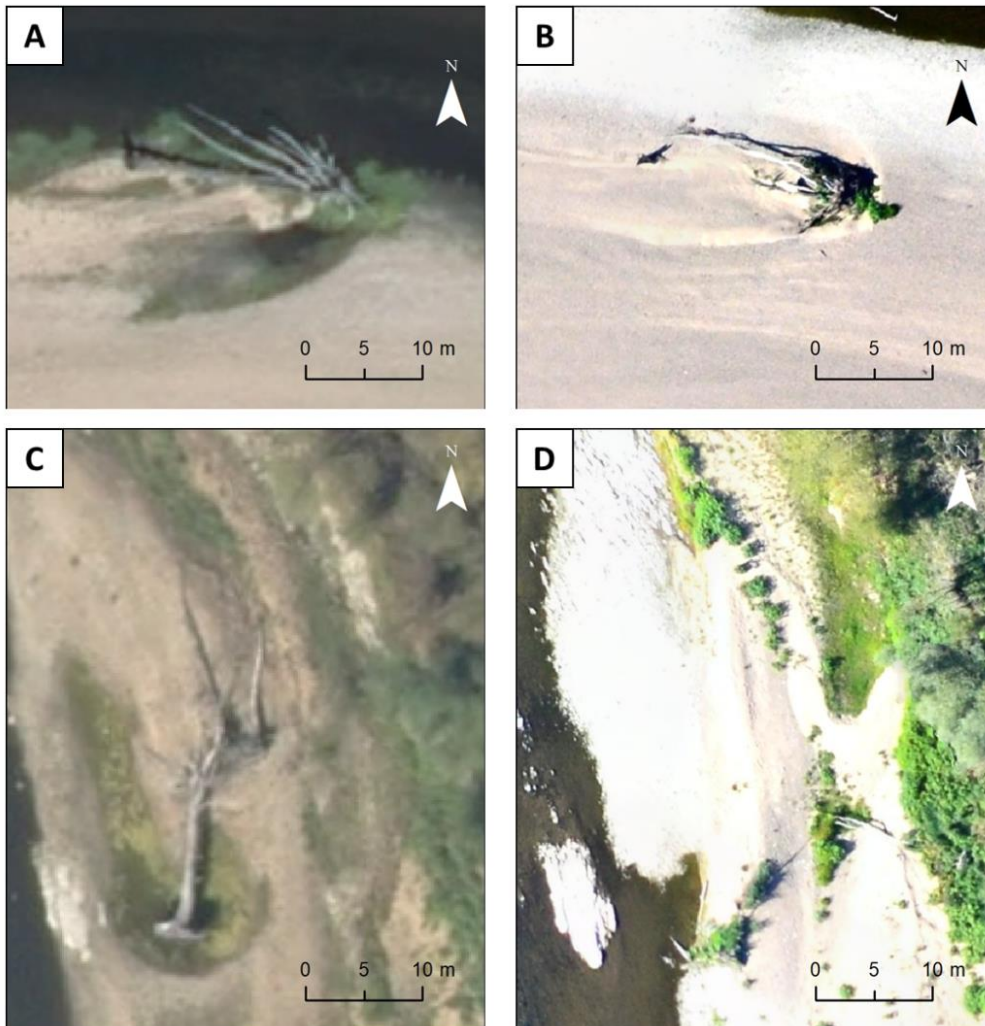
492

493 *Figure 7. Conceptual model summarising key results from this study.*

494 Most of the stable jams did not show significant changes in size between 2013 and 2020. This can
 495 be related to the relatively low maximum discharge, which fluctuated around Q_2 , and the increasing
 496 distance of jams from the river channel due to lateral erosion. Many jams seemed to decrease in size
 497 between 2013 and 2016, but their actual number was quite low, and vegetation colonisation over
 498 stable jams (as observed) can reduce visibility leading to false estimates of wood loss. Between 2019
 499 and 2020, a significantly higher number of jams expanded in size compared to other periods, in line
 500 with preferential organisation of wood into jam structures during the shorter biannual floods explained
 501 above. Even if the methods were adapted to reduce errors, it is possible that the jam size expansion
 502 would be overestimated when several wood pieces break down into smaller pieces within the same
 503 jam. At the same time, a stable jam can be considered as unchanged when the numbers of imported
 504 and exported pieces are equal. This situation was rarely observed in this case study. However, in
 505 some cases, a slight change in orientation or a few upstream pieces were noted without a global
 506 fluctuation in jam size.

507 On the braided Queets River in the U.S., wood export within a 5-year period was estimated at 50%
 508 (Latterell & Naiman, 2007). On the Arly and Isère Rivers, 60%–70% of wood pieces were remobilised,
 509 despite the absence of significant floods, which was not the case on the Arc River (France), which
 510 showed lower wood mobility over the same period (Piégay et al., 2017). An analysis based on multiple
 511 studies showed that the remobilisation rate of stored wood remained below 30% when discharge did
 512 not exceed bankfull level, and that export rates can reach 80% or higher at discharge equal to or
 513 exceeding bankfull level (Kramer & Wohl, 2017). In line with previous findings, the export rate of
 514 individual wood pieces in the Allier River was between 38% and 83%, and ranged from 40% to 86%

515 for jams. If we look at wood dynamics relative to wood imports, between 45% and 68% of newly
516 imported trunks are rapidly transported downstream within a timespan of one or three years
517 (depending on aerial image frequency). Monitoring mobility relative to wood import, allows the flood
518 history of imported wood pieces to be taken into account, and therefore allows the retention time to
519 be related to the hydrological conditions experienced by wood pieces during import and the
520 succeeding period until export conditions occur (if this happens within the studied period). It appears
521 that at least 45% (and up to 60%) of wood is exported from the reach by floods of lower, identical, or
522 slightly higher energy than the one that deposited it (Figure 3C). Whether wood is actually exported
523 can be questioned when high sediment deposition is observed. Wood can potentially be buried in
524 such cases, instead of being exported, but this phenomenon is difficult to accurately define on aerial
525 imagery (and sometimes even in the field). Some clues suggest that this situation happened between
526 2019 and 2020 (Figure 8), although we were unable to determine whether this is a common or
527 occasional process, and whether it is linked to specific hydrological conditions.



528

529 *Figure 8. Aerial photographs of two identical locations in (A) and (C) 2019, (B) and (D) 2020.*

530 We did not find a positive correlation between wood recruitment occurring through bank erosion and
531 increasing wood storage, as suggested by several authors (Kramer & Wohl, 2017), or between wood
532 storage and erosion rate (which considers all type of landcover). The wood import in 2016 was one
533 of the lowest recorded, despite the highest recruitment of wood through lateral erosion. Leaving 2010
534 out of the computation (very low flow conditions with low import), we observed an inverse tendency
535 compared with the one found in the literature: more individual pieces were imported and more jams
536 were built over periods characterised by low recruitment, which was an unexpected finding.
537 Furthermore, even though the highest erosion rate, associated with the highest flood magnitude, was
538 found during the period 2010–2013, wood import was virtually the same as over the period 2016–
539 2019. Our results indicate that events with high erosion capacity also have a high wood export
540 capacity. Conversely, Galia et al. (2023) observed a high individual wood export rate in association
541 with a lack of lateral erosion. This potentially means that, on the Allier River, wood influx originating
542 from local bank erosion is exported from the reach instead of being deposited nearby. The highest
543 wood import on the alluvial bars occurred in 2020, despite a low wood influx. We suggest several
544 explanations for this phenomenon.

- 545 (i) Wood influx was more important in the earlier years within reaches located upstream from
546 the study site, and the wood arrived in the study reach through a cascading process
547 (Lassetre et al., 2008; Piégay et al., 2017).
- 548 (ii) Several authors (Haga et al., 2002; Moulin & Piégay, 2004; Ruiz-Villanueva et al., 2019)
549 suggested that the order and frequency of flood occurrence play an important role, and
550 that two successive floods of similar magnitude do not always have the same effect on
551 wood mobility. In this study, we showed that flood duration also plays an important role in
552 the wood budget. The peak discharge in 2020 reached a higher level than in 2013, 2016,
553 and 2019, but the floods in 2020 and at the end of 2019 were of shorter duration (Figure
554 4). It has already been argued that flood duration can influence log transport distance
555 (Kramer & Wohl, 2017; Piégay et al., 2017; Ravazzolo et al., 2015), and thus that the
556 duration of flow above a critical discharge determines transport distance, rather than flow
557 magnitude (Piégay et al., 2017). If this is also the case on the Allier River, wood import
558 during shorter floods probably (at least partially) originated from nearby sources, as
559 demonstrated on the Tagliamento river (Bertoldi et al., 2013). The higher wood influx was
560 accompanied by a higher export rate during the earlier years: in 2020, even though wood
561 influx was low, the discharge conditions were not favourable to export of wood, but were
562 more beneficial to import of wood.
- 563 (iii) Another possible explanation is that the succession of floods of similar discharge (around
564 Q_2) and the decreasing flood length since 2016 have reinforced the filtering effect of wood

565 obstacles, thereby leading to positive feedback. Therefore, although a lower amount of
566 wood was introduced from the banks, the wood was deposited on alluvial bars, resulting
567 in an increase in the wood budget. Boivin et al. (2017a) suggested that individual wood
568 pieces introduced by high flow events are transported towards already existing jams during
569 subsequent floods. Once a logjam is formed, it then becomes an efficient trapping element
570 for individual wood logs (Dixon & Sear, 2014; Millington & Sear, 2007). A study by Pettit
571 et al. (2005) demonstrated that the majority of jams that are initiated by a key member
572 have a greater size than those that are not initiated by a key member. In line with this, the
573 number of jams increased after 2016, and since 2013, proportionally more wood was
574 stored within jams than was deposited in the form of individual logs. Furthermore, a one-
575 year duration with a complete absence of high flows preceded the floods of 2019–2020, a
576 situation that is very favourable to the generation of high wood flux (Zhang et al., 2021).
577 Moreover, the colonisation of alluvial bars by vegetation creates additional natural filters,
578 resulting in a situation where floods of around Q_2 are insufficient to remove wood. This is
579 clearly visible on the aerial images (Figure 1), where active channel width can be seen to
580 decrease over time, in line with the alluvial landscape dynamics of 1964 to 2000 (Petit,
581 2006). However, as explained earlier, the exact amount of wood filtered by riparian
582 vegetation cannot be estimated through analysis of aerial images.

583 Model simulations made by Ruiz-Villanueva et al. (2014) demonstrated that water depth over a
584 particular surface plays an important role in the control of wood deposition. In this context, the
585 exporting process can be hindered if positive biogeomorphic feedback between wood, sediment, and
586 living vegetation creates the conditions for the emergence of biogeomorphic units, which in turn lead
587 to rising topographic level (Collins et al., 2012; Corenblit et al., 2011; Gurnell, 2014). The increasing
588 amount of stabilised wood since 2013 is also a sign of an increasingly steady system. Considering
589 these findings in the context of climate change, we can ask the question whether longer low-flow
590 periods accompanied by an absence or low frequency of large floods result in an increased
591 opportunity to trap wood on bars and slow down its downstream export, with potential counter-effects
592 in terms of blockage at downstream-located infrastructure and overflowing in the case of smaller
593 rivers. Several studies (Curran, 2010; Wohl & Goode, 2008) revealed direct links between increasing
594 wood residence time or persistent jams and increased influence on ecology, channel hydraulics, and
595 geomorphology. We also showed that wood can remain stable over several years, depending on
596 hydrological conditions. Local conditions of sediment texture, topographic evolution, and water
597 temperature modification in relation to large wood should be analysed and related to habitat conditions
598 at variable channel gradients to achieve integrative river management solutions.

599 5. Conclusion

600 In this study, we determined how hydrological conditions control large wood dynamics within a 12-
601 km-long reach of the Allier River. Overall mobility patterns were found to be similar to those observed
602 in other studies at the basin scale, with features being shared between individual pieces and logjams.
603 Both flow magnitude and duration are important considerations when predicting wood import, export,
604 and storage, with there being three key parameters: $Q > Q_{bf}$, duration of peak flow, and $Q < 0.6Q_{bf}$.
605 Imported wood has, on average, a 50% chance of being remobilised immediately, depending on
606 whether relative discharge is positive (i.e., $Q_{remobilisation} > Q_{installation}$) or not. Jams are more durable
607 elements of the river landscape than isolated wood pieces, and about half of jams are built-up on so-
608 called key members. The Allier River shows a rather high density of large wood, and the stability of
609 wood deposits has risen over the last decade, with an increasingly high proportion of wood being
610 trapped in jams. It is likely that a potential positive feedback loop has occurred between wood,
611 sediment, and riparian vegetation, because the successive floods around Q_2 have progressively
612 increased stability. Knowledge on large wood mobility and the potential effects of wood on channel
613 morphology can be useful for river management actions, including wood reintroduction. Our
614 understanding of the retention time should be extended in future research with related habitat
615 analysis, which could help in the design of habitat restoration projects.

616

617 **Acknowledgements**

618 This work was supported by the French Biodiversity Agency (*Office Français de la Biodiversité*). The
619 project benefited from financial and technical support from Véodis-3D consulting agency. We thank
620 the Val d'Allier National Natural Reserve (*Réserve Natuelle National du Val d'Allier*) for their
621 substantial support for our project. This work was performed within the framework of the EUR
622 H₂O'Lyon (ANR-17-EURE-0018) of Université de Lyon, within the programme '*Investissements*
623 *d'Avenir*' operated by the French National Research Agency (ANR).

624

625 **Data Availability Statement**

626 The data that support the findings of this study are available from the corresponding author, BH, upon
627 reasonable request.

628

629 6. References

- 630 Abbe, T. B., & Montgomery, D. R. (1996). Large Woody Debris Jams, Channel Hydraulics and Habitat
631 Formation in Large Rivers. *Regulated Rivers: Research & Management*, 12(2-3), 201-221.
632 [https://doi.org/10.1002/\(SICI\)1099-1646\(199603\)12:2/3<201::AID-RRR390>3.0.CO;2-A](https://doi.org/10.1002/(SICI)1099-1646(199603)12:2/3<201::AID-RRR390>3.0.CO;2-A)
- 633 Andreoli, A., Comiti, F., & Lenzi, M. A. (2007). Characteristics, distribution and geomorphic role of
634 large woody debris in a mountain stream of the Chilean Andes. *Earth Surface Processes and*
635 *Landforms*, 32(11), 1675-1692. <https://doi.org/10.1002/esp.1593>
- 636 Atha, J. B. (2013). *Fluvial wood presence and dynamics over a thirty year interval in forested*
637 *watersheds*. University of Oregon.
- 638 Atha, J. B. (2014). Identification of Fluvial Wood Using Google Earth. *River Research and*
639 *Applications*, 30(7), 857-864. <https://doi.org/10.1002/rra.2683>
- 640 Benke, A., & Wallace, J. B. (2010). Influence of wood on invertebrate communities in streams and
641 rivers. In: Gregory, S.V.; Boyer, K.L; Gurnell, A.M. Eds. *The Ecology and Management of*
642 *Wood in World Rivers. American Fisheries Society, Symposium 37: Bethesda, Maryland. p.*
643 *149-177., 37, 149-177.*
- 644 Bertoldi, W., Gurnell, A. M., & Welber, M. (2013). Wood recruitment and retention : The fate of eroded
645 trees on a braided river explored using a combination of field and remotely-sensed data
646 sources. *Geomorphology*, 180-181, 146-155. <https://doi.org/10.1016/j.geomorph.2012.10.003>
- 647 Boivin, M., Buffin-Bélanger, T., & Piégay, H. (2015). The raft of the Saint-Jean River, Gaspé (Québec,
648 Canada) : A dynamic feature trapping most of the wood transported from the catchment.
649 *Geomorphology*, 231, 270-280. <https://doi.org/10.1016/j.geomorph.2014.12.015>

- 650 Boivin, M., Buffin-Bélanger, T., & Piégay, H. (2017a). Interannual kinetics (2010–2013) of large wood
651 in a river corridor exposed to a 50-year flood event and fluvial ice dynamics. *Geomorphology*,
652 279, 59-73. <https://doi.org/10.1016/j.geomorph.2016.07.010>
- 653 Boivin, M., Buffin-Bélanger, T., & Piégay, H. (2017b). Estimation of large wood budgets in a watershed
654 and river corridor at interdecadal to interannual scales in a cold-temperate fluvial system. *Earth*
655 *Surface Processes and Landforms*, 42(13), 2199-2213. <https://doi.org/10.1002/esp.4174>
- 656 Collins, B. D., Montgomery, D. R., Fetherston, K. L., & Abbe, T. B. (2012). The floodplain large-wood
657 cycle hypothesis : A mechanism for the physical and biotic structuring of temperate forested
658 alluvial valleys in the North Pacific coastal ecoregion. *Geomorphology*, 139-140, 460-470.
659 <https://doi.org/10.1016/j.geomorph.2011.11.011>
- 660 Comiti, F., Pecorari, E., Mao, L., Rigon, E., & Lenzi, M. A. (2008). *New methods for determining wood*
661 *storage and mobility in large gravel- bed rivers EPIC FORCE project (Deliverable D20bis)*.
662 <https://research.ncl.ac.uk/epicforce/assets/D20bis.pdf>
- 663 Corenblit, D., Baas, A. C. W., Bornette, G., Darrozes, J., Delmotte, S., Francis, R. A., Gurnell, A. M.,
664 Julien, F., Naiman, R. J., & Steiger, J. (2011). Feedbacks between geomorphology and biota
665 controlling Earth surface processes and landforms : A review of foundation concepts and
666 current understandings. *Earth-Science Reviews*, 106(3-4), 307-331.
667 <https://doi.org/10.1016/j.earscirev.2011.03.002>
- 668 Curran, J. C. (2010). Mobility of large woody debris (LWD) jams in a low gradient channel.
669 *Geomorphology*, 116(3-4), 320-329. <https://doi.org/10.1016/j.geomorph.2009.11.027>
- 670 Daniels, M. D. (2006). Distribution and dynamics of large woody debris and organic matter in a low-
671 energy meandering stream. *Geomorphology*, 77(3), 286-298.
672 <https://doi.org/10.1016/j.geomorph.2006.01.011>

- 673 Dixon, S. J., & Sear, D. A. (2014). The influence of geomorphology on large wood dynamics in a low
674 gradient headwater stream. *Water Resources Research*, 50(12), 9194-9210.
675 <https://doi.org/10.1002/2014WR015947>
- 676 Dunkerley, D. (2014). Nature and hydro-geomorphic roles of trees and woody debris in a dryland
677 ephemeral stream : Fowlers Creek, arid western New South Wales, Australia. *Journal of Arid*
678 *Environments*, 102, 40-49. <https://doi.org/10.1016/j.jaridenv.2013.10.017>
- 679 Elozegi, A., Díez, J., & Pozo, J. (2007). Contribution of dead wood to the carbon flux in forested
680 streams. *Earth Surface Processes and Landforms*, 32(8), 1219-1228.
681 <https://doi.org/10.1002/esp.1549>
- 682 Galia, T., Macurová, T., Vardakas, L., Škarpich, V., Matušková, T., & Kalogianni, E. (2020). Drivers
683 of variability in large wood loads along the fluvial continuum of a Mediterranean intermittent
684 river. *Earth Surface Processes and Landforms*, 45(9), 2048-2062.
685 <https://doi.org/10.1002/esp.4865>
- 686 Galia, T., Škarpich, V., Vardakas, L., Dimitriou, E., Panagopoulos, Y., & Spálovský, V. (2023).
687 Spatiotemporal variations of large wood and river channel morphology in a rapidly degraded
688 reach of an intermittent river. *Earth Surface Processes and Landforms*, esp.5531.
689 <https://doi.org/10.1002/esp.5531>
- 690 Galia, T., Tichavský, R., Wyżga, B., Mikuš, P., & Zawiejska, J. (2022). Assessing patterns of spatial
691 distribution of large wood in semi-natural, single-thread channels of Central Europe. *CATENA*,
692 215, 106315. <https://doi.org/10.1016/j.catena.2022.106315>
- 693 Ghaffarian, H., Piégay, H., Lopez, D., Rivière, N., MacVicar, B., Antonio, A., & Mignot, E. (2020).
694 Video-monitoring of wood discharge : First inter-basin comparison and recommendations to
695 install video cameras. *Earth Surface Processes and Landforms*, 45(10), 2219-2234.
696 <https://doi.org/10.1002/esp.4875>

- 697 Gregory, K. J., Gurnell, A. M., & Hill, C. T. (1985). The permanence of debris dams related to river
698 channel processes. *Hydrological Sciences Journal*, 30(3), 371-381.
699 <https://doi.org/10.1080/02626668509491000>
- 700 Guiney, M. R., & Lininger, K. B. (2022). Disturbance and valley confinement : Controls on floodplain
701 large wood and organic matter jam deposition in the Colorado Front Range, USA. *Earth*
702 *Surface Processes and Landforms*, 47(6), 1371-1389. <https://doi.org/10.1002/esp.5321>
- 703 Gurnell, A. M. (2014). Plants as river system engineers. *Earth Surface Processes and Landforms*,
704 39(1), 4-25. <https://doi.org/10.1002/esp.3397>
- 705 Gurnell, A. M., & Petts, G. E. (2002). Island-dominated landscapes of large floodplain rivers, a
706 European perspective. *Freshwater Biology*, 47(4), 581-600. <https://doi.org/10.1046/j.1365-2427.2002.00923.x>
- 707
- 708 Gurnell, A. M., Piégay, H., Swanson, F. J., & Gregory, S. V. (2002). Large wood and fluvial processes.
709 *Freshwater Biology*, 47(4), 601-619. <https://doi.org/10.1046/j.1365-2427.2002.00916.x>
- 710 Gurnell, A. M., & Sweet, R. (1998). The distribution of large woody debris accumulations and pools in
711 relation to woodland stream management in a small, low-gradient stream. *Earth Surface*
712 *Processes and Landforms*, 23(12), 1101-1121. [https://doi.org/10.1002/\(SICI\)1096-9837\(199812\)23:12<1101::AID-ESP935>3.0.CO;2-O](https://doi.org/10.1002/(SICI)1096-9837(199812)23:12<1101::AID-ESP935>3.0.CO;2-O)
- 713
- 714 Haga, H., Kumagai, T., Otsuki, K., & Ogawa, S. (2002). Transport and retention of coarse woody
715 debris in mountain streams : An in situ field experiment of log transport and a field survey of
716 coarse woody debris distribution. *Water Resources Research*, 38(8), 1-1-1-16.
717 <https://doi.org/10.1029/2001WR001123>
- 718 Haschenburger, J. K., & Rice, S. P. (2004). Changes in woody debris and bed material texture in a
719 gravel-bed channel. *Geomorphology*, 60(3), 241-267.
720 <https://doi.org/10.1016/j.geomorph.2003.08.003>

- 721 Hassan, M. A., Bird, S., Reid, D., & Hogan, D. (2016). Simulated wood budgets in two mountain
722 streams. *Geomorphology*, 259, 119-133. <https://doi.org/10.1016/j.geomorph.2016.02.010>
- 723 Iroumé, A., Cartagena, M., Villablanca, L., Sanhueza, D., Mazzorana, B., & Picco, L. (2020). Long-
724 term large wood load fluctuations in two low-order streams in Southern Chile. *Earth Surface*
725 *Processes and Landforms*, 45(9), 1959-1973. <https://doi.org/10.1002/esp.4858>
- 726 Iroumé, A., Mao, L., Andreoli, A., Ulloa, H., & Ardiles, M. P. (2015). Large wood mobility processes in
727 low-order Chilean river channels. *Geomorphology*, 228, 681-693.
728 <https://doi.org/10.1016/j.geomorph.2014.10.025>
- 729 Iroumé, A., Mao, L., Ulloa, H., Ruz, C., & Andreoli, A. (2014). Large Wood Volume and Longitudinal
730 Distribution in Channel Segments Draining Catchments with Different Land Use, Chile. *Open*
731 *Journal of Modern Hydrology*, 04(02), 57-66. <https://doi.org/10.4236/ojmh.2014.42005>
- 732 Jochner, M., Turowski, J. M., Badoux, A., Stoffel, M., & Rickli, C. (2015). The role of log jams and
733 exceptional flood events in mobilizing coarse particulate organic matter in a steep headwater
734 stream. *Earth Surface Dynamics*, 3(3), 311-320. <https://doi.org/10.5194/esurf-3-311-2015>
- 735 Jones, K. K., Anlauf-Dunn, K., Jacobsen, P. S., Strickland, M., Tennant, L., & Tippery, S. E. (2014).
736 Effectiveness of Instream Wood Treatments to Restore Stream Complexity and Winter
737 Rearing Habitat for Juvenile Coho Salmon. *Transactions of the American Fisheries Society*,
738 143(2), 334-345. <https://doi.org/10.1080/00028487.2013.852623>
- 739 Keller, E. A., & Swanson, F. J. (1979). Effects of large organic material on channel form and fluvial
740 processes. *Earth Surface Processes*, 4(4), 361-380. <https://doi.org/10.1002/esp.3290040406>
- 741 Kramer, N., & Wohl, E. (2015). Driftcretions: The legacy impacts of driftwood on shoreline
742 morphology. *Geophysical Research Letters*, 42(14), 5855-5864.
743 <https://doi.org/10.1002/2015GL064441>

- 744 Kramer, N., & Wohl, E. (2017). Rules of the road : A qualitative and quantitative synthesis of large
745 wood transport through drainage networks. *Geomorphology*, 279, 74-97.
746 <https://doi.org/10.1016/j.geomorph.2016.08.026>
- 747 Lassetre, N. S., Piégay, H., Dufour, S., & Rollet, A.-J. (2008). Decadal changes in distribution and
748 frequency of wood in a free meandering river, the Ain River, France. *Earth Surface Processes
749 and Landforms*, 33(7), 1098-1112. <https://doi.org/10.1002/esp.1605>
- 750 Latterell, J. J., & Naiman, R. J. (2007). Sources and dynamics of large logs in a temperate floodplain
751 river. *Ecological Applications*, 17(4), 1127-1141. <https://doi.org/10.1890/06-0963>
- 752 Le Lay, Y.-F., Moulin, B., & Piégay, H. (2013). Wood Entrance, Deposition, Transfer and Effects on
753 Fluvial Forms and Processes : Problem Statements and Challenging Issues. In *Treatise on
754 Geomorphology* (Vol. 12, p. 20-36). <https://doi.org/10.1016/B978-0-12-374739-6.00320-1>
- 755 Leckie, D. G., Cloney, E., Jay, C., & Paradine, D. (2005). Automated Mapping of Stream Features
756 with High-Resolution Multispectral Imagery. *Photogrammetric Engineering & Remote
757 Sensing*, 71(2), 145-155. <https://doi.org/10.14358/PERS.71.2.145>
- 758 Likens, G. E., & Bilby, R. (1982). Development, maintenance, and role of organic-debris dams in New
759 England streams. *Workshop on sediment budgets and routing in forested drainage basins:
760 proc.*, 122-128.
- 761 Máčka, Z., Krejčí, L., Loučková, B., & Peterková, L. (2011). A critical review of field techniques
762 employed in the survey of large woody debris in river corridors : A central European
763 perspective. *Environmental Monitoring and Assessment*, 181(1), 291-316.
764 <https://doi.org/10.1007/s10661-010-1830-8>
- 765 MacVicar, B. J., Piégay, H., Henderson, A., Comiti, F., Oberlin, C., & Pecorari, E. (2009). Quantifying
766 the temporal dynamics of wood in large rivers : Field trials of wood surveying, dating, tracking,

767 and monitoring techniques. *Earth Surface Processes and Landforms*, 34(15), 2031-2046.
768 <https://doi.org/10.1002/esp.1888>

769 MacVicar, B., & Piégay, H. (2012). Implementation and validation of video monitoring for wood
770 budgeting in a wandering piedmont river, the Ain River (France). *Earth Surface Processes and*
771 *Landforms*, 37(12), 1272-1289. <https://doi.org/10.1002/esp.3240>

772 Marcus, W. A., Marston, R. A., Colvard, C. R., & Gray, R. D. (2002). Mapping the spatial and temporal
773 distributions of woody debris in streams of the Greater Yellowstone Ecosystem, USA.
774 *Geomorphology*, 44(3-4), 323-335. [https://doi.org/10.1016/S0169-555X\(01\)00181-7](https://doi.org/10.1016/S0169-555X(01)00181-7)

775 Massé, S., & Buffin-Bélanger, T. (2016). Understanding hydrogeomorphological dynamics and the
776 distribution of large wood jams to promote sustainable river management strategies: In-
777 stream large wood jam dynamics. *The Canadian Geographer / Le Géographe Canadien*,
778 60(4), 505-518. <https://doi.org/10.1111/cag.12283>

779 Millington, C. E., & Sear, D. A. (2007). Impacts of river restoration on small-wood dynamics in a low-
780 gradient headwater stream. *Earth Surface Processes and Landforms*, 32(8), 1204-1218.
781 <https://doi.org/10.1002/esp.1552>

782 Moulin, B., & Piégay, H. (2004). Characteristics and temporal variability of large woody debris trapped
783 in a reservoir on the River Rhone (Rhone): Implications for river basin management. *River*
784 *Research and Applications*, 20(1), 79-97. <https://doi.org/10.1002/rra.724>

785 Moulin, B., Schenk, E. R., & Hupp, C. R. (2011). Distribution and characterization of in-channel large
786 wood in relation to geomorphic patterns on a low-gradient river. *Earth Surface Processes and*
787 *Landforms*, 36(9), 1137-1151. <https://doi.org/10.1002/esp.2135>

788 Petit, S. (2006). Reconstitution de la dynamique du paysage alluvial de trois secteurs fonctionnels de
789 la rivière Allier (1946-2000), Massif Central, France. *Géographie physique et Quaternaire*,
790 60(3), 271-287. <https://doi.org/10.7202/018000ar>

- 791 Pettit, N. E., Naiman, R. J., Rogers, K. H., & Little, J. E. (2005). Post-flooding distribution and
792 characteristics of large woody debris piles along the semi-arid Sabie River, South Africa. *River*
793 *Research and Applications*, 21(1), 27-38. <https://doi.org/10.1002/rra.812>
- 794 Pettit, N. E., Warfe, D. M., Kennard, M. J., Pusey, B. J., Davies, P. M., & Douglas, M. M. (2013).
795 Dynamics of in-stream wood and its importance as fish habitat in a large tropical floodplain
796 river: River wood and fish habitat. *River Research and Applications*, 29(7), 864-875.
797 <https://doi.org/10.1002/rra.2580>
- 798 Piégay, H. (1993). Nature, mass and preferential sites of coarse woody debris deposits in the lower
799 ain valley (Mollon reach), France. *Regulated Rivers: Research & Management*, 8(4), 359-372.
800 <https://doi.org/10.1002/rrr.3450080406>
- 801 Piégay, H., & Gurnell, A. M. (1997). Large woody debris and river geomorphological pattern :
802 Examples from S.E. France and S. England. *Geomorphology*, 19(1), 99-116.
803 [https://doi.org/10.1016/S0169-555X\(96\)00045-1](https://doi.org/10.1016/S0169-555X(96)00045-1)
- 804 Piégay, H., & Landon, N. (1997). Promoting ecological management of riparian forests on the Drôme
805 River, France. *Aquatic Conservation: Marine and Freshwater Ecosystems*, 7(4), 287-304.
806 [https://doi.org/10.1002/\(SICI\)1099-0755\(199712\)7:4<287::AID-AQC247>3.0.CO;2-S](https://doi.org/10.1002/(SICI)1099-0755(199712)7:4<287::AID-AQC247>3.0.CO;2-S)
- 807 Piégay, H., & Marston, R. A. (1998). Distribution of large woody debris along the outer bend of
808 meanders in the Ain river, France. *Physical Geography*, 19(4), 318-340.
809 <https://doi.org/10.1080/02723646.1998.10642654>
- 810 Piégay, H., Moulin, B., & Hupp, C. R. (2017). Assessment of transfer patterns and origins of in-channel
811 wood in large rivers using repeated field surveys and wood characterisation (the Isère River
812 upstream of Pontcharra, France). *Geomorphology*, 279, 27-43.
813 <https://doi.org/10.1016/j.geomorph.2016.07.020>

814 Piégay, H., Thévenet, A., & Citterio, A. (1999). Input, storage and distribution of large woody debris
815 along a mountain river continuum, the Drôme River, France. *CATENA*, 35(1), 19-39.
816 [https://doi.org/10.1016/S0341-8162\(98\)00120-9](https://doi.org/10.1016/S0341-8162(98)00120-9)

817 R Core Team. (2022). *A language and environment for statistical computing*. R Foundation for
818 Statistical Computing. <https://www.R-project.org/>

819 Ravazzolo, D., Mao, L., Picco, L., & Lenzi, M. A. (2015). Tracking log displacement during floods in
820 the Tagliamento River using RFID and GPS tracker devices. *Geomorphology*, 228, 226-233.
821 <https://doi.org/10.1016/j.geomorph.2014.09.012>

822 Richardson, J. J., & Moskal, L. M. (2016). An Integrated Approach for Monitoring Contemporary and
823 Recrutable Large Woody Debris. *Remote Sensing*, 8(9), Article 9.
824 <https://doi.org/10.3390/rs8090778>

825 Ruiz-Villanueva, V., Bodoque, J. M., Díez-Herrero, A., & Bladé, E. (2014). Large wood transport as
826 significant influence on flood risk in a mountain village. *Natural Hazards*, 74(2), 967-987.
827 <https://doi.org/10.1007/s11069-014-1222-4>

828 Ruiz-Villanueva, V., Mazzorana, B., Bladé, E., Bürkli, L., Iribarren-Anacona, P., Mao, L., Nakamura,
829 F., Ravazzolo, D., Rickenmann, D., Sanz-Ramos, M., Stoffel, M., & Wohl, E. (2019).
830 Characterization of wood-laden flows in rivers : Wood-laden flows. *Earth Surface Processes
831 and Landforms*, 44(9), 1694-1709. <https://doi.org/10.1002/esp.4603>

832 Ruiz-Villanueva, V., Piégay, H., Gurnell, A. M., Marston, R. A., & Stoffel, M. (2016). Recent advances
833 quantifying the large wood dynamics in river basins : New methods and remaining challenges.
834 *Reviews of Geophysics*, 54(3), 611-652. <https://doi.org/10.1002/2015RG000514>

835 Ruiz-Villanueva, V., Wyżga, B., Hajdukiewicz, H., & Stoffel, M. (2016). Exploring large wood retention
836 and deposition in contrasting river morphologies linking numerical modelling and field

- 837 observations. *Earth Surface Processes and Landforms*, 41(4), 446-459.
838 <https://doi.org/10.1002/esp.3832>
- 839 Schenk, E. R., Moulin, B., Hupp, C. R., & Richter, J. M. (2014). Large wood budget and transport
840 dynamics on a large river using radio telemetry. *Earth Surface Processes and Landforms*,
841 39(4), 487-498. <https://doi.org/10.1002/esp.3463>
- 842 Schmocker, L., & Hager, W. H. (2011). Probability of Drift Blockage at Bridge Decks. *Journal of*
843 *Hydraulic Engineering*, 137(4), 470-479. [https://doi.org/10.1061/\(ASCE\)HY.1943-](https://doi.org/10.1061/(ASCE)HY.1943-7900.0000319)
844 7900.0000319
- 845 Senter, A., Pasternack, G., Piégay, H., & Vaughan, M. (2017). Wood export prediction at the
846 watershed scale. *Earth Surface Processes and Landforms*, 42(14), 2377-2392.
847 <https://doi.org/10.1002/esp.4190>
- 848 Smikrud, K. M., & Prakash, A. (2006). Monitoring Large Woody Debris Dynamics in the Unuk River,
849 Alaska Using Digital Aerial Photography. *GIScience & Remote Sensing*, 43(2), 142-154.
850 <https://doi.org/10.2747/1548-1603.43.2.142>
- 851 Ulloa, H., Iroumé, A., Mao, L., Andreoli, A., Diez, S., & Lara, L. E. (2015). Use of remote imagery to
852 analyse changes in morphology and longitudinal large wood distribution in the Blanco River
853 after the 2008 Chaitén volcanic eruption, southern Chile. *Geografiska Annaler. Series A,*
854 *Physical Geography*, 97(3), 523-541.
- 855 Wohl, E. (2013). Floodplains and wood. *Earth-Science Reviews*, 123, 194-212.
856 <https://doi.org/10.1016/j.earscirev.2013.04.009>
- 857 Wohl, E., & Cadol, D. (2011). Neighborhood matters : Patterns and controls on wood distribution in
858 old-growth forest streams of the Colorado Front Range, USA. *Geomorphology*, 125(1),
859 132-146. <https://doi.org/10.1016/j.geomorph.2010.09.008>

- 860 Wohl, E., Dwire, K., Sutfin, N., Polvi, L., & Bazan, R. (2012). Mechanisms of carbon storage in
861 mountainous headwater rivers. *Nature Communications*, 3(1), Article 1.
862 <https://doi.org/10.1038/ncomms2274>
- 863 Wohl, E., & Goode, J. R. (2008). Wood dynamics in headwater streams of the Colorado Rocky
864 Mountains: WOOD DYNAMICS IN COLORADO. *Water Resources Research*, 44(9).
865 <https://doi.org/10.1029/2007WR006522>
- 866 Zhang, Z., Ghaffarian, H., MacVicar, B., Vaudor, L., Antonio, A., Michel, K., & Piégay, H. (2021). Video
867 monitoring of in-channel wood : From flux characterization and prediction to recommendations
868 to equip stations. *Earth Surface Processes and Landforms*, 46(4), 822-836.
869 <https://doi.org/10.1002/esp.5068>
870